

Exhibit C  
09/720,086

## Alanine Scanning Mutagenesis of Insulin\*

(Received for publication, December 24, 1996, and in revised form, February 28, 1997)

Claus Kristensen†§, Thomas Kjeldsen†, Finn C. Wiberg†, Lauge Schäffer†, Morten Hachl, Svend Havelund†, Joseph Bass\*\*, Donald F. Steiner†§§, and Asser S. Andersen†

From the Departments of †Insulin Research, ‡Cell Technology, and ‖Protein Chemistry, Novo Nordisk, 2880 Bagsvaerd, Denmark, the \*\*Department of Medicine, Section of Endocrinology, the ‡‡Department of Biochemistry and Molecular Biology, and the §§Howard Hughes Medical Institute, University of Chicago, Chicago, Illinois 60637

Alanine scanning mutagenesis has been used to identify specific side chains of insulin which strongly influence binding to the insulin receptor. A total of 21 new insulin analog constructs were made, and in addition 7 high pressure liquid chromatography-purified analogs were tested, covering alanine substitutions in positions B1, B2, B3, B4, B8, B9, B10, B11, B12, B13, B16, B17, B18, B20, B21, B22, B26, A4, A8, A9, A12, A13, A14, A15, A16, A17, A19, and A21. Binding data on the analogs revealed that the alanine mutations that were most disruptive for binding were at positions TyrA19, GlyB8, LeuB11, and GluB13, resulting in decreases in affinity of 1,000-, 33-, 14-, and 8-fold, respectively, relative to wild-type insulin. In contrast, alanine substitutions at positions GlyB20, ArgB22, and SerA9 resulted in an increase in affinity for the insulin receptor. The most striking finding is that B20Ala insulin retains high affinity binding to the receptor. GlyB20 is conserved in insulins from different species, and in the structure of the B-chain it appears to be essential for the shift from the  $\alpha$ -helix B8–B19 to the  $\beta$ -turn B20–B22. Thus, replacing GlyB20 with alanine most likely modifies the structure of the B-chain in this region, but this structural change appears to enhance binding to the insulin receptor.

Insulin mediates its effects by binding to the insulin receptor in the plasma membrane of target cells. The molecular mechanisms for insulin interaction with the receptor are not fully understood. The crystal structure of the insulin molecule has been known for more than 25 years (1), but it remains an open question whether the structure of insulin that binds to the receptor is similar to the crystal structure. Until the structure of bound insulin and the side chains that are actually involved in binding is identified by co-crystallization of the receptor and ligand, more information about the binding domain on insulin can be obtained using mutational approaches.

The binding domain of the insulin molecule has been studied by investigating receptor binding of a number of insulins from different animal species as well as chemically modified and more recently genetically engineered insulins (2–4). These studies have provided experimental support for a model in which invariant residues from both A and B chains form a surface that binds to the insulin receptor. The putative binding domain comprises a number of residues overlapping the dimer-forming surface (ValB12, TyrB16, GlyB23, PheB24, PheB25,

TyrB26, GlyA1, GlnA5, TyrA19, and AsnA21) and some of the residues buried beneath the COOH terminus of the B-chain (IleA2, ValA3, GluA4) (2). Cross-linking studies with an azido-phenylalanine-substituted analog have shown that one of these residues, PheB25, comes into close proximity to the insulin receptor upon binding (5).

Recently, a second binding site has been proposed, involving residues LeuA13 and LeuB17 (6, 7). A biphasic binding reaction involving this second binding site could explain the negative cooperativity phenomenon (8) as well as discrepancies between receptor binding data and metabolic potencies found in hystericomorph insulins and synthetic analogs with mutations at these positions (9, 10).

Although a large number of insulin analogs have been studied to date, no comprehensive analysis of the insulin side chains involved in receptor binding has been reported. We have applied alanine scanning mutagenesis to elucidate further the role of individual amino acid residues in receptor binding. A total of 21 new insulin constructs with alanine substitutions were expressed as single chain insulin precursors in the yeast *Saccharomyces cerevisiae*. Yeast culture medium was treated with *Achromobacter lyticus* protease to yield mature insulin and then used directly in the binding assay. The receptor used for the binding assay is an IR<sup>1</sup>-IgG fusion protein immobilized in microtiter plates coated with protein A.

The binding affinity of 19 new analogs and 7 HPLC-purified alanine analogs was measured. Compiling these data with data in the literature on alanine analogs allows an extensive overview covering the effect of single alanine substitutions at a total of 38 positions of the insulin molecule. We conclude that insulin residue TyrA19 is essential for binding to receptor, whereas single alanine mutations in the B20–B22 turn actually appear to enhance affinity for insulin receptor.

### MATERIALS AND METHODS

**Miscellaneous**—Insulin, A14-<sup>125</sup>I-insulin, and *A. lyticus* protease were from Novo Nordisk. DNA restriction enzymes and T4 ligase were from New England Biolabs. Taq polymerase was from Perkin-Elmer. *Staphylococcus aureus* protein A, Sepharose FF for immobilizing *A. lyticus* protease, and the SP-Sepharose BigBeads were from Pharmacia Biotech Inc.

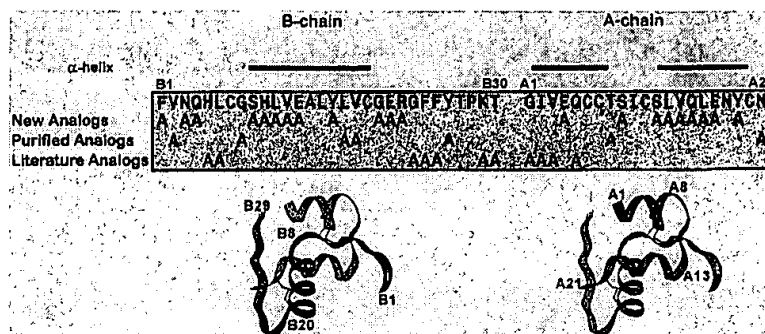
**Vector Construction and Expression in Yeast**—Single alanine mutations were inserted in the sequence encoding insulin precursor by polymerase chain reaction or overlap polymerase chain reaction using appropriate oligonucleotides (11). The polymerase chain reaction fragment was purified and subcloned into the yeast expression vector cPOT using standard procedures (12). The yeast expression system used has been described in detail previously (13). Briefly, the insulin precursor was coupled to a 41-amino acid synthetic prepropeptide sequence in the configuration: prepropeptide-KR-extension-insulin precursor, where KR is the potential Kex2 protease processing site, the extension is the removable spacer peptide E(EA)<sub>3</sub>EPK, and the insulin precursor is

\* The costs of publication of this article were defrayed in part by the payment of page charges. This article must therefore be hereby marked "advertisement" in accordance with 18 U.S.C. Section 1734 solely to indicate this fact.

† To whom correspondence should be addressed: Insulin Research, Novo Nordisk, Novo Allé 6B1.74, 2880 Bagsvaerd, Denmark. Tel.: 45-4442-3572; Fax: 45-4444-4250.

<sup>1</sup> The abbreviations used are: IR, insulin receptor; HPLC, high pressure liquid chromatography.

**FIG. 1. Overview of insulin analogs with single alanine substitution.** Amino acid sequence of insulin with positions of alanine substitutions indicated by A. New analogs and purified analogs (HPLC-purified) are described under "Materials and Methods." Literature analogs have been described previously (1, 22–26).



either minipinsulin B(1–29)-A(1–21) or B(1–29)-AAK-A(1–21) (14, 15). Thus the precursors are single chain proinsulin-like peptides that either lack the C-peptide or have the short synthetic C-peptide AAK.

The insulin precursor constructs were expressed in *S. cerevisiae* strain MT663 (16). Yeast cells were transformed and selected on YP plates with 2% glucose according to standard methods (17). Yeast cultures were grown in YP medium with 2% glucose for 72 h at 30 °C, and the yield of insulin precursor in the fermentation supernatants was quantified by HPLC with human insulin as external standard (18).

**Enzymatic Conversion of Insulin Precursors**—The single chain insulin precursors were converted to des-B30-insulin using the lysine-specific *A. lyticus* endoprotease that removes the extension and the C-peptide of the precursor. Cell-free yeast culture medium with precursor was adjusted to pH 9 with 0.1 volume 0.5 M glycine, pH 9, and applied to a column with *A. lyticus* protease immobilized on Sepharose. The column was incubated for 2 h at 37 °C before cleaved precursor was eluted from column into 0.1 volume of 1 M Tris, pH 7.0, and the concentration of des-B30-insulin was quantified by HPLC (18).

For analogs that were expressed poorly the precursor was partially purified by cation exchange chromatography prior to treatment with *A. lyticus* protease. Briefly, the cell-free yeast medium was adjusted to pH 3.0 with HCl and then batch treated with cation exchange resin (SP-Sepharose BigBeads) for 16 h at room temperature to adsorb peptides, which were subsequently eluted with 200 mM NaCl, 50 mM glycine, pH 9.0. The HPLC-purified analogs (B2Ala, B8Ala, B17Ala, B18Ala, B26Ala, A8Ala, and A21Ala) were fermented in yeast and purified as described (4, 14).

**Insulin Receptor Binding Assay**—The insulin receptor used is a soluble fusion protein consisting of the insulin receptor (exon 11+) ectodomain fused to the Fc region of the IgG heavy chain (19). The IR-IgG fusion was stably expressed in baby hamster kidney cells by inserting the 3,532-base pair *NotI/XbaI* fragment from the pBluescript II-HIRs-Fc vector (19) into the ZEM expression vector and transfecting this into baby hamster kidney cells as described previously (20, 21).

For binding experiments the IR-IgG fusion protein was immobilized on protein A-coated microtiter plates. First the wells were coated with protein A by incubating for 1 h with 50  $\mu$ l of protein A (1  $\mu$ g/ml) in TBS (150 mM NaCl, 10 mM Tris, pH 7.5); then the plates were washed three times with binding buffer (100 mM Hepes, pH 8.0, 100 mM NaCl, 10 mM MgCl<sub>2</sub>, 0.5% (w/v) bovine serum albumin, 0.025% (w/v) Triton X-100). The IR-IgG fusion receptor was immobilized by adding 50  $\mu$ l of a 33-fold dilution of baby hamster kidney supernatant in binding buffer to each well and incubating for 3 h before washing the plates three times with binding buffer. Binding experiments were performed by adding a total volume of 150  $\mu$ l of binding buffer with A14-<sup>125</sup>I-insulin (10 pM) and varying dilutions of *A. lyticus* protease-treated insulin analog. After 16 h at 4 °C unbound ligand was removed by aspirating the buffer and washing once with 200  $\mu$ l of cold binding buffer, and the radioactivity in each well was counted. The concentration of receptor in the well was adjusted to yield 10–15% binding when no competing ligand was added in the assay.

The data from the competitive displacement experiments were fitted to a two-site binding model using a nonlinear regression algorithm in GraphPad Prism 2.01 (GraphPad Software, San Diego). All sets of binding data fitted better to the two-site model than the one-site model.

## RESULTS

**Alanine Constructs and Expression in Yeast**—For the alanine scanning mutagenesis we made 21 new insulin analog constructs with alanine substitutions in positions B1, B3, B4, B9, B10, B11, B12, B13, B16, B20, B21, B22, A4, A9, A12, A13,

A14, A15, A16, A17, and A19 (Fig. 1). We chose these 21 positions because they are located primarily on the surface of the insulin molecule and therefore are more likely to be candidates involved in receptor binding.

The insulin precursors were expressed in the yeast *S. cerevisiae* and fermented in 5-ml cultures. The yield of insulin precursor in the fermentation supernatant was quantified on HPLC. The yield of the alanine analog precursors relative to the wild-type insulin precursor is shown in Fig. 2. Most of the alanine substitutions result in some decrease in yield, probably because the yeast expression system is optimized for expressing the wild-type insulin precursor. Nevertheless, 15 of the analogs gave more than 20% of the yield of the wild-type precursor, indicating that they are processed and folded correctly by the yeast cell. The positions where the alanine substitutions had the most deleterious effects on expression levels were at the hydrophobic residues LeuB11, ValB12, and LeuA16. Mutations in the region GlyB20, GluB21, and ArgB22 also resulted in poor yields, indicating that the precursor is folded less efficiently because of structural changes induced by alanine mutations in this region.

Because of the low level of expression the B11Ala, B12Ala, and A16Ala insulin analogs were partially purified using cation exchange chromatography. The B20Ala and B22Ala analog data were obtained from both partially purified and raw medium supernatants. Two of the insulin analogs (B12Ala and A16Ala) never yielded sufficient material for binding experiments.

The precursors were converted to des-B30-insulin by treating with *A. lyticus* protease. HPLC chromatograms for the wild-type insulin precursor before and after *A. lyticus* protease treatment are shown in Fig. 3. The *A. lyticus* protease-treated precursor elutes later from the HPLC column than untreated precursor because of increased hydrophobicity, and this allowed precise quantification of the converted precursor.

**Receptor Binding**—For the binding assay an IR-IgG fusion protein was immobilized in microtiter plates using protein A. This binding assay allows efficient analyses of the high number of analogs, and in addition this assay has lower background than precipitation assays. The binding data obtained when displacing A14-<sup>125</sup>I-insulin from the IR-IgG receptor with insulin standard (Fig. 4A) fits to a two-site binding model and yields binding affinities (ED<sub>50</sub>) of 0.012 and 1.4 nM for the two predicted sites. However, the 0.012 nM value for the high affinity site is not reliable because it is similar to the concentration of tracer added (10 pM), and therefore all binding data presented reflect binding to the low affinity site, that is, affinities in the range of 0.3–200 nM. The binding affinity of each analog is based on at least three independent sets of binding curves.

Binding of the wild-type insulin precursor expressed in the yeast cells before and after treatment with *A. lyticus* protease is included in Fig. 4A. The affinity of the wild-type precursor after *A. lyticus* protease treatment (des-B30-insulin) is similar

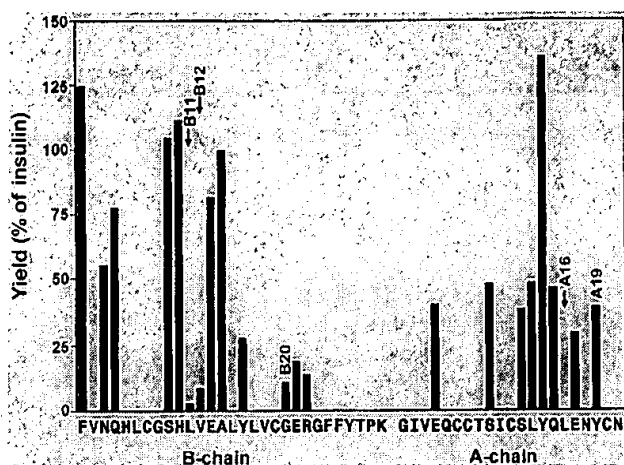


FIG. 2. Yield of insulin analogs with alanine mutation. The figure shows the yield of mutated precursor relative to the yield of wild-type insulin precursor for each position of alanine substitution. The yeast *S. cerevisiae* was transformed with cPOT plasmid carrying cDNA encoding mutated insulin precursor. The yield of precursors was quantified by HPLC.

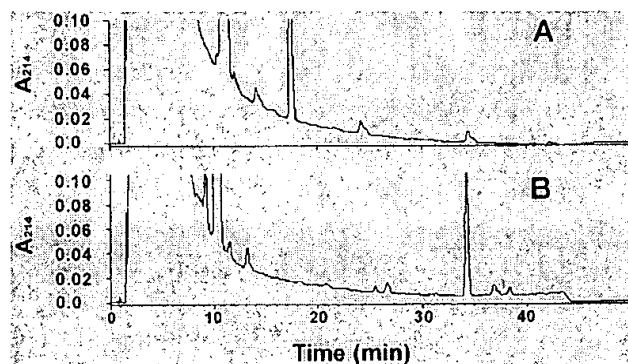


FIG. 3. HPLC analysis of insulin precursor. Chromatograms showing the HPLC elution profile after applying culture supernatant from yeast expressing wild-type insulin precursor. In panel A the supernatant was untreated, and in panel B the supernatant was converted to des-B30-insulin by treating with *A. lyticus* protease (panel B).

to the affinity of insulin ( $ED_{50}$  0.016 and 1.5 nM), whereas the curve for the uncleaved insulin precursor is shifted far to the right (Fig. 4A), demonstrating a very poor affinity of the uncleaved precursor for the insulin receptor. This is consistent with previous reports on the biological activity of the miniprotein B(1–29)-A(1–21) (15). The assay was further verified when measuring affinities of the HPLC-purified analogs. Five of these have been investigated previously, and the relative affinities obtained for the IR-IgG and the full-length insulin receptor are similar<sup>2</sup> (Table I). These controls demonstrate that the *in vitro* IR-IgG binding assay performed directly on *A. lyticus* protease-treated yeast culture supernatants reproduces previous assays using the full-length receptor.

In all of the binding experiments performed the purified insulin and the wild-type precursor were included as standards, and all data are expressed as the  $ED_{50}$  of analog relative to the  $ED_{50}$  of the wild-type insulin precursor.

Three analogs tested showed a marked decrease in affinity for the receptor, supporting a role for these residues in receptor binding. The most pronounced decrease occurred with TyrA19 → Ala. We could not obtain a full binding curve due to the poor affinity; the curve for the A19Ala analog is shifted about three

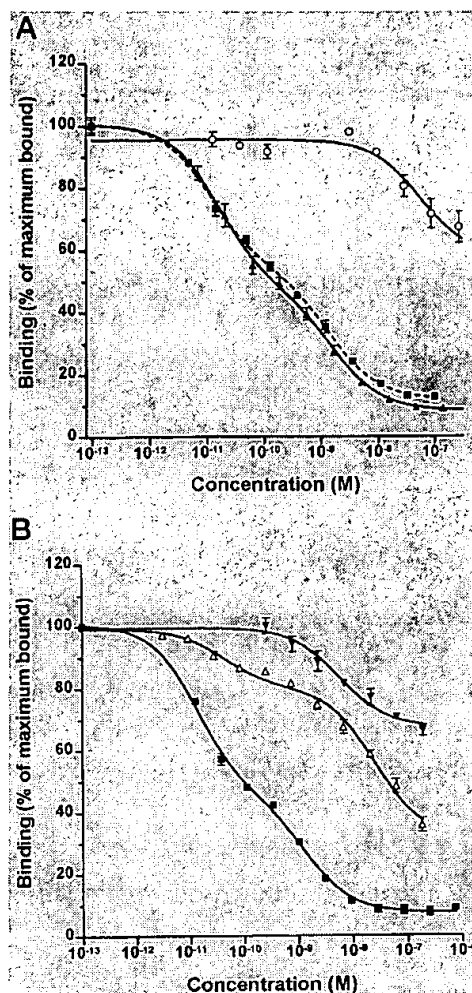


FIG. 4. Competition curves for  $^{125}$ I-insulin binding to insulin receptor. IR-IgG receptor immobilized in microtiter plates was incubated with  $^{125}$ I-insulin (10 pM) for 16 h at 4 °C together with varying dilutions of unlabeled analog. The amount of  $^{125}$ I-insulin bound, as a percentage of  $^{125}$ I-insulin bound in the absence of unlabeled analog, is plotted against the concentration of unlabeled analog. Panel A,  $^{125}$ I-insulin displaced with insulin ( $\blacktriangle$ ), *A. lyticus* protease-treated wild-type insulin precursor ( $\blacksquare$ ), or untreated wild-type insulin precursor ( $\circ$ ). Panel B,  $^{125}$ I-insulin displaced with the following three *A. lyticus* protease-treated precursors: wild-type insulin ( $\blacksquare$ ), B11Ala insulin ( $\triangle$ ), or A19Ala insulin ( $\blacktriangledown$ ).

decades to the right compared with the wild-type insulin curve (Fig. 4B), implying a 1,000-fold decreased affinity for the insulin receptor. Other disruptive alanine substitutions were found at LeuB11 and GluB13, resulting in a drop to 7 and 12%, respectively, in affinity for the receptor (Fig. 4B). One of the HPLC-purified analogs, B8Ala insulin, also disrupted binding, with an approximate decrease of 30-fold in affinity for the receptor. Although residues LeuA13 and LeuB17 have been suggested to be part of a second binding site in the insulin molecule, alanine substitutions at these positions had only modest effect on the binding affinity (2–3-fold) (Table I).

In contrast to the disruptive mutations there were a number of alanine substitutions that did not alter affinity for the receptor, and at least three of the alanine analogs even showed an increase in receptor affinity. Alanine substitution for residues GlyB20, ArgB22, and SerA9 consistently resulted in a 2–4-fold increase in affinity for the insulin receptor (Table I).

The binding data are summarized in Table I and Fig. 5. When including data on alanine analogs reported in the liter-

<sup>2</sup> L. Schäfer, unpublished data.

TABLE I  
Alanine scanning receptor binding data

Shown is a summary of binding data on alanine-substituted insulin analogs. For each analog the average of relative affinities  $\pm$  S.D. for at least three independent experiments is shown. The data were determined from binding curves similar to those shown in Fig. 4, as described under "Materials and Methods." For analogs described in the literature the data represent relative receptor binding affinity except for B5Ala and A5Ala insulins where data are lipolysis potencies in fat cells (24).

A-chain				B-chain			
Position		Affinity experimentally determined	Affinity reported in literature	Position		Affinity experimentally determined	Affinity reported in literature
		% of insulin	% of insulin			% of insulin	% of insulin
A1	G		12 (22)	B1	F	79 $\pm$ 26	
A2	I		0.6 (23)	B2	V	110 $\pm$ 21	
A3	V		1.8 (23)	B3	N	134 $\pm$ 21	
A4	E	139 $\pm$ 35		B4	Q	54 $\pm$ 16	
A5	Q		49 (24)	B5	H		31 (24)
A6	C	—		B6	L		1.4 (25)
A7	C	—		B7	C	—	
A8	T	87 $\pm$ 13	78 <sup>a</sup>	B8	G	3 $\pm$ 2	
A9	S	260 $\pm$ 87		B9	S	80 $\pm$ 23	
A10	I	—		B10	H	80 $\pm$ 24	
A11	C	—		B11	L	7 $\pm$ 1	
A12	S	108 $\pm$ 28		B12	V	—	
A13	L	30 $\pm$ 7		B13	E	12 $\pm$ 3	
A14	Y	66 $\pm$ 13		B14	A	—	110 (insulin)
A15	Q	122 $\pm$ 37		B15	L	—	
A16	L	—		B16	Y	69 $\pm$ 15	
A17	E	56 $\pm$ 20		B17	L	62 $\pm$ 14	24 <sup>a</sup>
A18	N	—		B18	V	88 $\pm$ 17	35 <sup>a</sup>
A19	Y	0.1		B19	C	—	
A20	C	—		B20	G	270 $\pm$ 85	
A21	N	66 $\pm$ 5	140 <sup>a</sup>	B21	E	230 $\pm$ 79	
				B22	R	405 $\pm$ 187	
				B23	G		3 (26)
				B24	F		5 (26)
				B25	F		10 (26)
				B26	Y	36 $\pm$ 8	64 <sup>a</sup>
				B27	T	—	
				B28	P	—	
				B29	K		76 (34)
				B30	T		102 (porcine insulin)

<sup>a</sup> L. Schäffer, unpublished data.

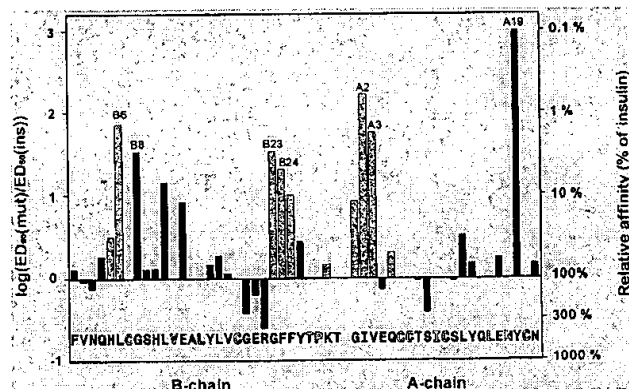


FIG. 5. Overview of alanine scanning receptor binding data. The binding data are shown as relative affinity versus position of mutation. Black bars are binding data measured in the present study, and the gray bars are data reported in the literature (22–26). The amino acid sequence of insulin is shown at the bottom; for the amino acids printed in white no data on alanine-substituted analog are available. All data represent receptor binding affinity (22, 23, 25, 26), except for the data on B5Ala and A5Ala insulins, which are lipolysis potencies in fat cells (24).

ature (1, 22–26) the effects of alanine substitutions at a total of 38 positions of the insulin molecule are now available.

#### DISCUSSION

By implementing a new high volume screening assay for insulin analogs we have used the alanine scanning mutagenesis approach to identify amino acid side chains of insulin which

strongly influence binding to the insulin receptor. A total of 21 single alanine mutants of insulin were expressed in yeast and converted to des-B30-insulin using *A. lyticus* endoprotease. The binding constants of the analogs for the IR-IgG fusion receptor were determined in a microtiter plate assay based on immobilization of receptor using protein A. This receptor retains high affinity for insulin (19), and immobilization via protein A does not influence binding affinity (data not shown).

In the present study the binding affinity of 19 new analogs and 7 HPLC-purified analogs was measured. Compiling these data with analogs described in the literature allows an extensive overview covering the effect of substituting alanine at 38 positions of the insulin molecule (Table I and Fig. 5).

Two types of information are obtained in this mutagenesis study. First, mutations that disrupt binding are of interest because they indicate that the residue of insulin either interacts directly with the receptor or, alternatively, that the residue supports a conformation required for receptor binding. Additionally, scanning mutagenesis provides a test to confirm the role of residues thought to be essential for receptor binding. If alanine substituted at these positions does not alter binding, the structure in this particular region does not appear to be important for binding.

In addition to binding data, comparison of analog yields in the *S. cerevisiae* expression system reveals differences in the biosynthesis of the analogs. Most of the alanine-substituted analogs were expressed efficiently; 15 of the analogs gave more than 20% of the yield of the wild-type precursor, indicating that these analogs were folded efficiently by the yeast cell (Fig. 2). The positions where the alanine substitution had the most

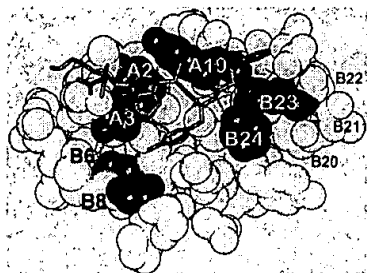


FIG. 6. Crystal structure of insulin molecule. Shown is a space-filling model of insulin; residues important for receptor binding are shown in black. Alanine substitution for these residues reduces affinity for receptor more than 20-fold. The proposed receptor binding patch consisting of amino acids GlyB23, PheB24, IleA2, ValA3, and TyrA19 (white labels) is partly covered by the COOH terminus of the B-chain. For clarity the COOH terminus of the B-chain (B25–B30) is shown as sticks in the figure. Residues GlyB8 and LeuB6 (gray labels) are probably important for the structure of insulin; B6 is located on the opposite side of the insulin molecule. The residues of the B20–B22 turn are labeled; substituting alanine at these positions appear to improve affinity for insulin receptor. The structure of insulin T-conformation was obtained from the Protein Data Bank (PDB); Brookhaven data base (33), and visualized using RasMol software.

deleterious effect on expression level were at the hydrophobic residues LeuB11, ValB12, and LeuA16. These amino acids are buried in the hydrophobic core of the insulin molecule and therefore might provide the free energy needed for efficient folding. Poor yields were also observed in analogs with mutations in the loop region B20–B22 (Fig. 2).

Binding data on the new analogs revealed that the alanine mutations that were most disruptive for binding were at positions TyrA19, LeuB11, and GluB13, resulting in decrease in affinity to 0.1, 7, and 12%, respectively, relative to wild-type insulin (Table I). The A19Ala analog is well expressed in the yeast expression system (Fig. 2), indicating that the folding is not altered by this mutation, pointing to a direct role of TyrA19 in interaction with the receptor. Three modifications of insulin at position A19 have been described previously (27–29). Replacing TyrA19 with leucine had a dramatic effect on receptor binding, decreasing the affinity 1,000-fold, whereas substitution with phenylalanine only resulted in a 4–5-fold decrease in affinity (27, 29). Additionally, iodination at TyrA19 had an intermediate effect on receptor binding (for review, see Ref. 28). Thus the substitution of alanine or leucine at position A19 disrupts receptor binding, whereas iodination or insertion of another aromatic ring at position A19 (Phe) is well tolerated, suggesting that an aromatic ring at position A19 is crucial for insulin binding to its receptor.

Including analogs reported in the literature (Table I) the alanine mutations that cause the largest reduction in binding are found at positions LeuB6, GlyB8, GlyB23, PheB24, IleA2, ValA3, and TyrA19. Substitution of alanine at these positions reduced affinity for the receptor by more than 20-fold (Table I). All of these residues are evolutionary conserved in insulins from different species, supporting the conclusion that they are important for structure and/or function. Most of these disruptive alanine mutations are related to the classical binding surface. The residues that are most likely to be directly involved in binding are B23, B24, and A19, which play a role in dimer formation, and A2 and A3, which are hydrophobic residues buried beneath the COOH terminus of the B-chain (Fig. 6). We propose that the residues that are essential for direct interaction with the receptor are found in this patch, but there may also be structural effects that can account for the disruption of binding when replacing these residues with alanine. In particular, interaction between A2 and A19 appears to stabilize the insulin conformation (30). Mutating one of these residues

thus could distort the conformation of insulin that binds to the receptor. On the other hand, the high expression yield of the A19Ala analog argues against major conformational distortions in this molecule.

The explanation for the large reduction in receptor affinity in insulin analogs LeuB6Ala and GlyB8Ala is not clear. A glycine residue is not likely to contribute free energy of binding, and in addition GlyB8 is thought to be important for initiating the central  $\alpha$ -helix of the B-chain. Therefore, mutating this residue probably has structural consequences. The B6Ala insulin was described by Nakagawa and Tager (25), and they also speculated on a structural role for the LeuB6 in insulin.

Substituting alanine for other residues of the classical putative binding surface including GluA4, AsnA21, TyrB16, and TyrB26 only altered affinity for the insulin receptor moderately (less than 3-fold) (Table I), indicating that these residues are not part of the functional binding epitope.

These data are incorporated in the structural model shown in Fig. 6. The five residues GlyB23, PheB24, IleA2, ValA3, and TyrA19 form a patch in the insulin molecule. Substituting alanine for any of these five amino acids results in more than a 20-fold decrease in receptor affinity, and therefore we propose that this patch is essential for direct interaction with the insulin receptor. In the structure of insulin, part of this proposed binding patch is buried beneath the COOH terminus of the B-chain; if all of these residues interact directly with the receptor partial unfolding of the COOH-terminal B-chain would be required for exposing this patch. Such a mechanism would be in accordance with the hypothesis of Dodson and others that some degree of separation of COOH-terminal B-chain from  $\text{NH}_2$ -terminal A-chain is required for interaction with the insulin receptor (15, 31).

Two recent papers have suggested that in addition to the classical binding site there is a second binding site in the hexamer-forming surface of the insulin molecule (6, 7). This second binding surface includes LeuA13 and LeuB17. In the present study alanine substitutions at these positions did not dramatically decrease affinity for the insulin receptor, the affinities of the A13Ala and B17Ala analogs were 30 and 52%, respectively (Table I). However, as we only look at the low affinity site of the IR-IgG fusion we may miss effects of A13 and B17 mutations. This would be in agreement with Schäffer (6), who reported that a characteristic of analogs mutated in positions A13 or B17 is that they bind with relative higher affinity to the soluble insulin receptor (nanomolar affinity site) than to the high affinity site of the holo-receptor (picomolar affinity) (6). Thus it would be expected that mutations in the second binding site would have less impact on binding to the low affinity site on the insulin receptor.

Three of the alanine substitutions resulted in a 2–4-fold increase in affinity for the insulin receptor fusion. These were SerA9Ala, ArgB22Ala, and most surprisingly GlyB20Ala (Table I). The expression yield of B20Ala and B22Ala was very low (Fig. 2) indicating that substituting alanine at these positions has structural consequences. GlyB20 is conserved in insulins from different species, but apparently it is not important for binding; thus it would be interesting to investigate the effect of the GlyB20Ala mutation on folding of the wild-type precursor proinsulin. In the structure of the insulin B-chain GlyB20 appears to be essential for the shift from the  $\alpha$ -helix B8–B19 to the  $\beta$ -turn B20–B22 (Fig. 6). Analyzing the impact of alanine at position B20 on the secondary structure of an insulin B-chain using the Chou-Fasman algorithm (32) suggests that the  $\alpha$ -helix B8–B19 will be extended by an additional turn comprising B20Ala, GluB21, and ArgB22. This does not take into account the interaction with the A-chain, but substituting glycine at

position B20 with alanine nevertheless is expected to cause conformational changes in this region. What effect this putative structural change could have on the COOH terminus of the B-chain is uncertain. Earlier reports on the natural mutation of PheB24 to serine (insulin Los Angeles) suggested that unfolding of the B-chain is compatible with high affinity receptor binding (31); it may be that similar effects will be seen when the structure of the B20Ala insulin is solved.

In conclusion, the present activity data on series of analogs will in combination with structure elucidation of selected analogs further characterize the functional properties of the insulin molecule.

**Acknowledgments**—We thank Durita Simonsen, Ulla M. Jørgensen, and Marianne Kallesøe for excellent technical assistance; Knud Vad for the B1Ala-insulin construct; and Per Balschmidt for the *A. lyticus* protease-Sepharose.

## REFERENCES

- Adams, M. J., Blundell, T. L., Dodson, E. J., Dodson, G. G., Vijayan, M., Baker, E. N., Harding, M. M., Hodgkin, D. C., Rimmer, R., and Sheet, S. (1969) *Nature* **224**, 491–496
- Baker, E. N., Blundell, T. L., Cutfield, J. F., Cutfield, S. M., Dodson, E. J., Hodgkin, D. M. C., Hubbard, R. E., Isaacs, N. W., Reynolds, C. D., Sakabe, K., Sakabe, N., and Vijayan, N. M. (1988) *Philos. Trans. R. Soc. Lond. Biol. Sci.* **319**, 369–456
- Gliemann, J., and Gammeltoft, S. (1974) *Diabetologia* **10**, 105–113
- Brange, J., Ribbel, U., Hansen, J. F., Dodson, G., Hansen, M. T., Havelund, S., Melberg, S. G., Norris, F., Norris, K., Snel, L., Sørensen, A. R., and Voigt, H. O. (1988) *Nature* **333**, 679–682
- Kurose, T., Pashmforoush, M., Yoshimasa, Y., Carroll, R., Schwartz, G. P., Burke, G. T., Katsoyannis, P. G., and Steiner, D. F. (1994) *J. Biol. Chem.* **269**, 29190–29197
- Schäffer, L. (1994) *Eur. J. Biochem.* **221**, 1127–1132
- De Meyts, P. (1994) *Diabetologia* **37**, S135–S148
- De Meyts, P., Roth, J., Neville, D. M. J., Gavin, J. R. I., and Lesniak, M. (1973) *Biochem. Biophys. Res. Commun.* **55**, 154–161
- Horuk, R., Goodwin, P., O'Connor, K., Neville, R. W. J., Lazarus, N. R., and Stone, D. (1979) *Nature* **279**, 439–440
- Bajaj, M., Blundell, T. L., Horuk, R., Pitts, J. E., Wood, S. P., Gowan, L. K., Schwabe, C., Wollmer, A., Gliemann, J., and Gammeltoft, S. (1986) *Biochem. J.* **238**, 345–351
- Ho, S. N., Hunt, H. D., Horton, R. M., Pullen, J. K., and Pease, L. R. (1989) *Gene (Amst.)* **77**, 51–59
- Sambrook, J., Fritsch, E. F., and Maniatis, T. (1989) *Molecular Cloning: A Laboratory Manual*, 2nd ed., Cold Spring Harbor Laboratory, Cold Spring Harbor, NY
- Kjeldsen, T., Brandt, J., Andersen, A. S., Egel-Mitani, M., Hach, M., Petterson, A. F., and Vad, K. (1996) *Gene (Amst.)* **170**, 107–112
- Markussen, J., Damgaard, U., Diers, I., Fiil, N., Hansen, M. T., Larsen, P., Norris, F., Norris, K., Schou, O., Snel, L., Thim, L., and Voigt, H. O. (1987) in *Peptides 1986* (Theodoropoulos, D., ed) pp. 190–194, Walter de Gruyter and Co. Berlin
- Derewenda, U., Derewenda, Z., Dodson, E. J., Dodson, G. G., Bing, X., and Markussen, J. (1991) *J. Mol. Biol.* **220**, 425–433
- Thim, L., Hansen, M. T., Norris, K., Hoegh, I., Boel, E., Forstrom, J., Ammerer, G., and Fiil, N. P. (1986) *Proc. Natl. Acad. Sci. U. S. A.* **83**, 6766–6770
- Sherman, F., Fink, G. R., and Lawrence, C. W. (1979) *Methods in Yeast Genetics: A Laboratory Manual*, Cold Spring Harbor Laboratory, Cold Spring Harbor, NY
- Kristensen, C., Andersen, A. S., Hach, M., Wiberg, F. C., Schäffer, L., and Kjeldsen, T. (1995) *Biochem. J.* **305**, 981–986
- Bass, J., Kurose, T., Pashmforoush, M., and Steiner, D. F. (1996) *J. Biol. Chem.* **271**, 19367–19375
- Andersen, A. S., Kjeldsen, T., Wiberg, F. C., Christensen, P. M., Rasmussen, J. S., Norris, K., Møller, K. B., and Møller, N. P. H. (1990) *Biochemistry* **29**, 7363–7366
- Kjeldsen, T., Andersen, A. S., Wiberg, F. C., Rasmussen, J. S., Schäffer, L., Balschmidt, P., Møller, K. B., and Møller, N. P. H. (1991) *Proc. Natl. Acad. Sci. U. S. A.* **88**, 4404–4408
- Cosmatos, A., Cheng, K., Okada, Y., and Katsoyannis, P. G. (1978) *J. Biol. Chem.* **253**, 6586–6590
- Nakagawa, S. H., and Tager, H. S. (1992) *Biochemistry* **31**, 3204–3214
- Marki, F., Gasparo, M. D., Eisler, K., Kamber, B., Riniker, B., Rittel, W., and Sieber, P. (1979) *Hoppe-Seyler's Z. Physiol. Chem.* **360**, 1619–1632
- Nakagawa, S. H., and Tager, H. S. (1991) *J. Biol. Chem.* **266**, 11502–11509
- Kobayashi, M., Ohgaku, S., Iwasaki, M., Maegawa, H., Watanabe, N., Takada, Y., Shigeta, Y., and Inouye, K. (1984) *Biomed. Res.* **5**, 267–272
- Kitagawa, K., Ogawa, H., Thomson Burke, G., Chanley, J. D., and Katsoyannis, P. G. (1984) *Biochemistry* **23**, 4444–4448
- Gammeltoft, S. (1984) *Physiol. Rev.* **64**, 1322–1378
- Federigios, N., Thomson Burke, G., Kitagawa, K., and Katsoyannis, P. G. (1983) *J. Protein Chem.* **2**, 147–170
- Derewenda, U., Derewenda, Z., Dodson, G. G., and Hubbard, R. E. (1990) in *Handbook of Experimental Pharmacology* (Cuatrecasas, P., and Jacobs, S., eds) pp. 23–39, Springer-Verlag, Berlin
- Hua, Q. X., Shoelson, S. E., Kochoyan, M., and Weiss, M. A. (1991) *Nature* **354**, 238–241
- Chou, P. Y., and Fasman, G. D. (1978) *Adv. Enzymol.* **47**, 45–148
- Smith, G. D., Swenson, D. C., Dodson, E. J., Dodson, G. G., and Reynolds, C. D. (1984) *Proc. Natl. Acad. Sci. U. S. A.* **81**, 7093–7097
- Mirmira, R. G., and Tager, H. S. (1991) *Biochemistry* **30**, 8222–8229